Li-Ion Battery-Supercapacitor Hybrid Storage System for a Long Lifetime, Photovoltaic-Based Wireless Sensor Network

Fabio Ongaro, Stefano Saggini, and Paolo Mattavelli, *Senior Member, IEEE*

***Abstract*—This paper proposes a power management architecture that utilizes both supercapacitor cells and a lithium battery as energy storages for a photovoltaic (PV)-based wireless sensor network. The supercapacitor guarantees a longer lifetime in terms of charge cycles and has a large range of operating temperatures, but has the drawback of having low energy density and high cost. The lithium battery has higher energy density but requires an accurate charge profile to increase its lifetime, feature that cannot be easily obtained supplying the wireless node with a fluctuating source as the PV one. Combining the two storages is possible to obtain good compromise in terms of energy density. A statistic analysis is used for sizing the storages and experimental results with a 5-W PV energy source are reported.**

***Index Terms*—Batteries, battery management systems, energy harvesting, energy management, energy storage, hybrid power systems, photovoltaic systems, supercapacitors.**

I. Introduction

A WIRELESS sensor network consists of a large number of microsensors distributed in an area of interest. Each node is used for environmental monitoring networks, military target tracking, and detection of chemical and biological weapons [1], and shares these informations with the other neighbouring nodes by using a wireless link. Ideally each node should be energy autonomous and without the need of battery replacement and disposal. In many application scenarios, the targeted node lifetime ranges, typically from 2 to 5 years, and the need of energy harvesting is a primary issue in order to grant effectiveness of the wide-spread diffusion of this technology. While a wide variety of harvesting modalities are now feasible, solar energy harvesting through photovoltaic (PV) conversion provides the highest power density, which makes it the preferred choice to power an embedded system that consumes severalmilliwatt using a reasonably small harvesting module [2]. Solar cells exhibit a strong nonlinear electrical characteristic and the extraction of energy is even more difficult in nonstationary environments. Variable operating conditions can be associated with the weather change (e.g., cloudy and nonoptimally radiating solar power environments) and ageing effects or efficiency degradation in the solar panel (e.g., dust or rust in the cell surface). Moreover, the energy transfer mechanism is strongly influenced by the illumination condition such as the angle of incidence of the sunlight that varies along the day especially if the sensor node is in a mobile system, besides shadows that depend also on the instantaneous position of the sensor. A simple and low cost way to extract and store energy from a PV source is to connect the solar panel directly to a battery with a diode [3], as shown in Fig. 1(a). The main disadvantage of this solution is that the system does not always work in the optimal condition to convert the available solar energy. To improve the system performance, a controller can be added between the PV panel and the battery [2]–[4], as shown in Fig. 1(b). The controller is usually a dc–dc converter and controls the input voltage or current so that the extracted energy is maximized, and the output voltage is fixed by another dc–dc converter; in the case of using a supercap as energy storage [5], the scheme is shown in Fig. 1(c) and generally the output converter is a step-up converter because of the low voltage of the supercapacitors. Maximum power point tracking (MPPT) circuits differentiate themselves in the design of the power converting electronics and/or in the control strategy, but the charging of batteries in presence of fluctuating power sources remains an open issue. For example, Fig. 2 reports the power obtainable by

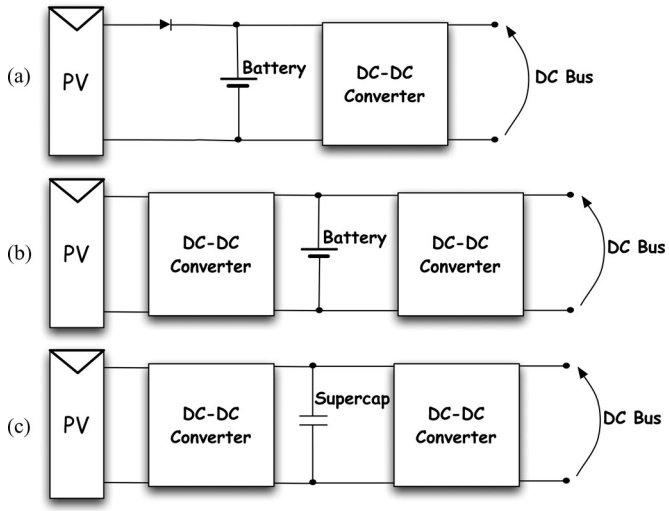

Fig. 1. Standard solutions for solar energy harvesting.

Manuscript received April 27, 2011; revised September 19, 2011 and December 19, 2011; accepted February 8, 2012. Date of current version May 15, 2012. Recommended for publication by Associate Editor F. Wang.

F. Ongaro is with the Department of Electrical, Mechanical and Management Engineering, University of Udine, Udine 33100, Italy, and also with the Texas Instruments Incorporated, Freising D-85356, Germany (e-mail: fabio.ongaro@uniud.it).

S. Saggini is with the Department of Electrical, Mechanical and Management Engineering, University of Udine, Udine 33100, Italy (e-mail: stefano.saggini@uniud.it).

P. Mattavelli is with the Center for Power Electronics Systems, Virginia Tech, Blacksburg, VA 24061 USA (e-mail: mattavelli@ieee.org).

Color versions of one or more of the figures in this paper are available online at http://ieeexplore.ieee.org.

Digital Object Identifier 10.1109/TPEL.2012.2189022

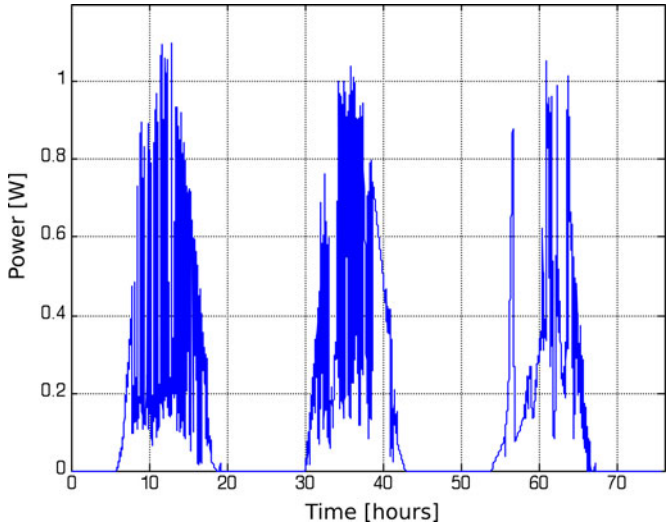

Fig. 2. Power obtainable by a PV of 2-W nominal power in a mobile system constituted by a buoy on the sea.

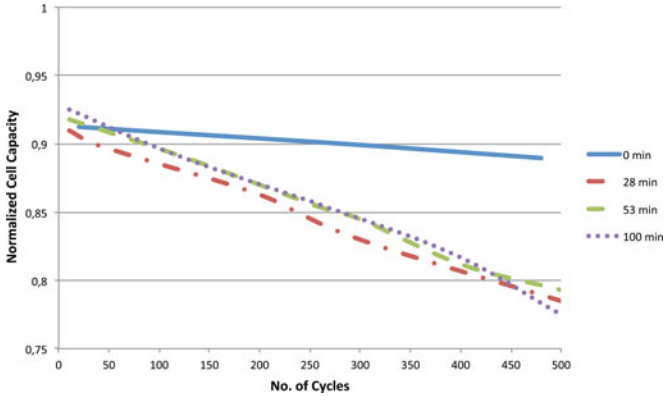

Fig. 3. Effect of constant voltage charge period at 4.2 V on cycle performance (data extracted from [6]). Test cells charged at constant current at 1-C rate to 4.2 V followed by the constant voltage float charging at this voltage for various periods and then discharged to 2.75 V at 1 C rate.

a PV panel, having 2 W as the nominal power, in a mobile system constituted by a buoy on the sea. As can be observed, even if the weather condition is good, the irradiation is in tropical condition, and the temperature is maintained stable by the water, the available power has a large fluctuation due to the wave motion that changes the instantaneous orientation. This situation is incompatible with the charging of high-density accumulators, like the lithium batteries, where a precise charge mechanism is required to preserve the lifetime of the battery [2], [6]–[11], which is generally composed by a constant current phase and a constant voltage phase.

Two choices are available for energy storage [2]: batteries and electrochemical double layer capacitors, also known as supercapacitors; batteries are a relatively mature technology and have a higher energy density (more capacity for a given volume, weight, and cost) than supercapacitors; however, supercapacitors have a higher power density than batteries, and are more efficient and offer higher lifetime in terms of charge-discharge cycles. The main disadvantage of supercapacitors in energy harvesting applications is the high leakage current.

This paper proposes a hybrid accumulator architecture that combines the advantages of the supercapacitors in terms of lifetime and charge/discharge cycles (10 years and millions of charge–discharge cycles [12]) and the lithium batteries for their highest energy density and costs; the power management is addressed to increase the lifetime of the storages, especially the lifetime of the Li-ion battery, which is typically the bottleneck of endurance in energy autonomous sensor nodes. One major contribution of this paper is also the statistical sizing strategy of the energy storage elements (i.e., the Li-ion battery and the supercap), that ensures a specified percentage of working time of the remote sensors during the year.

II. Degradation Mechanisms in Li-ion Batteries

Four types of rechargeable batteries are commonly used: nickel cadmium (NiCD), nickel metal hydride (NiMH), lithium based (Li+), and sealed lead acid (SLA) [2]. Of these, SLA and NiCD batteries are less used because the former has a relatively low energy density and weight, and the latter suffers from capacity loss caused by shallow discharge cycles, termed as the memory effect. The choice between NiMH and Li+ batteries became evident: Li+ batteries are more efficient than NiMH, have a longer cycle lifetime, involve a lower rate of self-discharge, and its cycle-life is independent of the Depth of discharge problem that is present also in SLA and NiCD batteries [6].

For better understanding the charge strategy used in the proposed architecture, it is useful to explain the mechanism that affects the lifetime of the Li-ion batteries. In general terms, the charge procedure consists of two phases: a constant current phase and a constant voltage phase; the charge current is expressed as a rate of the nominal capacitance, for example, charging a battery of 1000 mAh with a current of 1 A, means charging at 1 C; this phase requires the 20–30% of the charging time and allows the 70–80% of the total charge [10]. This state ends when the maximum cell voltage is reached (generally 4.2 V), and the second phase starts. In this last phase (constant voltage phase), the cell voltage is maintained until the current drops under the minimum current, that depends on the C rating of the battery or for a certain period of time. This last stage requires the 70–80% of the total time and allows the 20–30% of the total charge, but a long float-charge period at 4.2 V or above is one of the causes of the lifetime reduction of the cell [6], as shown in Fig. 3, whose values are obtained from real experiments made by [6] on a LiCoO2 cell. Another factor of degradation in Li-ion batteries is the high charge rate, i.e., > 0.5 C, this can be shown in Fig. 4 (results from [6]). At low charge rates < 0.5 C the degradation generally is independent of the charge rate.The worst degradation factor is the overvoltage condition: as can be seen in Fig. 5 (results from [6]), charging the battery at a voltage above the nominal voltage causes a rapid decrease of the overall capacity. From this consideration, it is possible to obtain some guidelines for the optimal solar battery charger for increasing the lifetime of the Li-ion cells.

1) The constant current phase, or CC, should be done at a low current rating (< 0.5 C), condition not always guaranteed

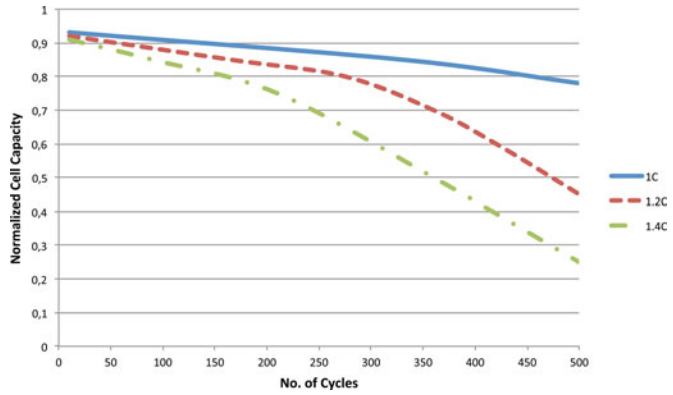

Fig. 4. Effect of charge rate on cycle performance (data extracted from [6]). Test cells charged at constant current at various rates to 4.2 V followed by constant voltage float charging at 4.2 V for 2.5 h and then discharged to 2.75 V at 1-C rate.

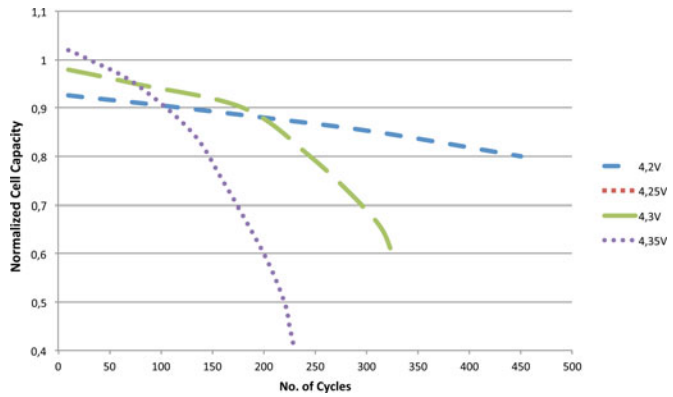

Fig. 5. Effect of constant voltage charge voltage on cycle performance (data extracted from [6]). Test cells charged at constant current at 1 C rate to cutoff voltage followed by constant voltage float charging at this voltage for 2.5 h and then discharged to 2.75 V at 1 C rate.

in a solar battery charger, it depends on the nominal power of the PV module and on the instantaneous irradiation.

2) The CC stage should stop if the nominal voltage is exceeded.
3) The constant voltage stage should be avoided. The drawback of this choice is loosing a part of the capacity of the battery (20–30%).
4) The number of charge/discharge cycles should be as low as possible. As previously explained the current coming directly from a PV cell due to the weather conditions is not constant. Quite often as a result of cloud formations passing in front of the sun, the current will be fluctuating. The result of this fluctuating input current is a recharging sequence that is quite often interrupted. The battery is charged for a while but before it is fully charged it is already partially used or discharged. Whether this is causing capacity fading is not clear. Note, however, that these cycles are shallow discharge cycles and small discharges and pulsed charging are sometimes claimed to enhance battery lifetime [11]. In this paper, only complete charge/discharge cycles are considered: the total charge stored in the battery is integrated and then divided for the nominal energy of the battery:

$$n_{\text{cycles}} = \frac{\int E_{\text{charge}}(t)\,\mathrm{d}t}{E_{\text{battery}}}. \tag{1}$$

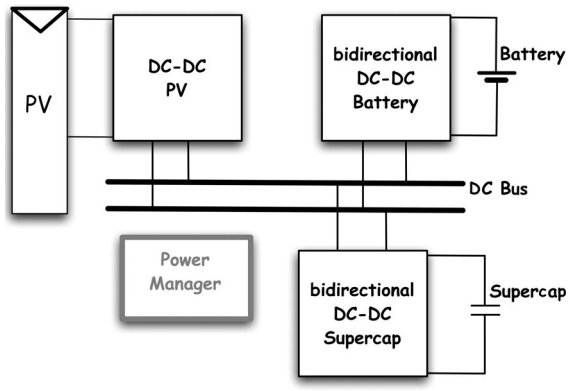

Fig. 6. Architecture of the proposed power management.

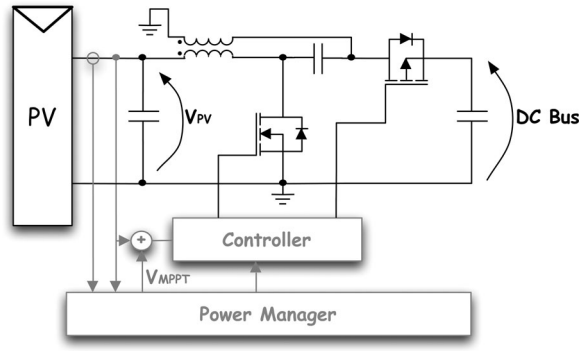

Fig. 7. Sepic converter utilized for PV conversion with input voltage controller.

III. Power Management Architecture and Control

The proposed power management architecture is reported in Fig. 6, where three dc–dc converters are connected in parallel to the dc power bus. The first converter, denoted dc–dc PV, interfaces the PV panel to the dc power bus, the second, denoted dc–dc battery, connects the dc bus to the battery, and the third, denoted dc–dc Supercap, connects the dc bus to the supercapacitors. The internal power bus is the main power supply of the electronic systems utilized by sensor node. The dc–dc PV converter realizes the MPPT of the PV module; the input voltage of the converter is controlled by a feedback loop and the reference is determined either by the source MPPT or by the control on the supercapacitor voltage, depending on the state of the power management algorithm. The dc–dc PV converter is based on a synchronous Sepic topology as reported in Fig. 7; this solution guarantees small input current ripple and it is compatible with the voltage of our PV cell (about 5 V) because, in CCM operation, the conversion ratio can be stepped down to the bus voltage, which is 3.3 V

$$\frac{V_{\text{BusDC}}}{V_{\text{PV}}} = \frac{D}{1-D} \tag{2}$$

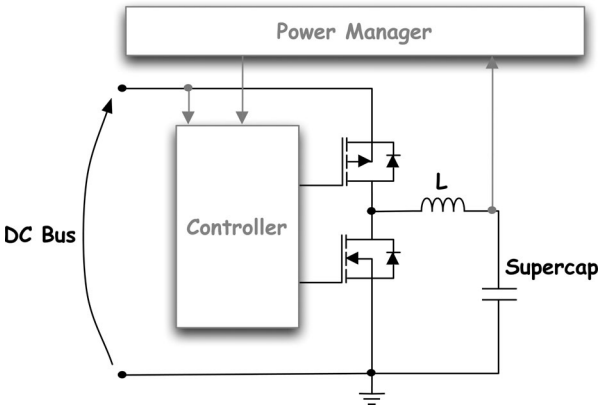

Fig. 8. Bidirectional buck converter connected to the supercapacitor.

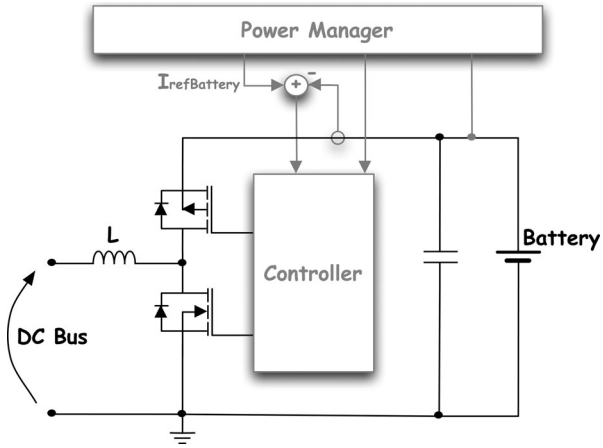

Fig. 9. Bidirectional boost converter connected to the battery.

The dc–dc supercap converter is a bidirectional converter synchronous buck converter reported in Fig. 8; several bidirectional, high-efficiency converters are present in the literature, also specifically for battery applications [15]–[18], [22], but for cell balancing in high-energy battery packs, or for interface supercaps and batteries to a high voltage (tens of volts), high power (hundreds of watts) dc bus, they require several switches, magnetic components or complex controls, that do not easily enable high efficiencies at low loads (milliwatts) like in our application. For this reason, a simple buck converter has been chosen. The converter operates in step-down mode when the current flows to the supercapacitor, and in step-up mode when energy from the supercapacitor is needed, being the typical maximum voltage of a supercap about 2.7/2.5 V [12]. This converter controls the dc bus voltage operating as a sink or a source depending on the instantaneous power budget of the system as explained in next section. The proposed architecture presents a direct power conversion from the solar panel to the load bus. The extra power available on the bus, due the difference between the source and load power, is stored in the supercapacitor and can be utilized by the conversion system when a reduction of the available power on the source is present. The stored energy can be designed to manage the variation of the instantaneous power guaranteeing the power to the load in a portable system, to supply the system for many hours without irradiation, or provide the energy necessary for charging the battery in case of fluctuation of the input power [13], [19]–[21]. By utilizing the bidirectional dc–dc converter, the supercapacitors are connected in parallel without requiring an over voltage protection system on each element that is needed in the serial connection as in [14]. The dc–dc battery converter is a bidirectional boost converter, as shown in Fig. 9, to charge and to utilize the battery at the same time depending on the working conditions. This choice is dictated by the required voltage level of the battery, respect to the dc power bus, in fact the lithium battery has a nominal voltage of 4.2 V and the dc bus voltage is 3.3 V. This converter operates like the dc–dc supercap converter, but has a current controlled loop, and the power management algorithm decides the current reference based on the charging/discharging state of the battery.

The power management algorithm is basically based on six different states. In the first stage, the Off" stage, all the storages are discharged, the controller is in sleep state, and all the converters are disabled; when the energy provided from the solar module is sufficient for power the controllers, a startup procedure occurs. If the input power is sufficient the algorithm moves to the "Soft Start" stage; the "dc–dc PV" converter starts to control the input voltage and the controller provides the voltage reference for realizing the MPPT, the "dc–dc Supercap" controls the voltage of main dc bus and the energy difference between the input solar panel and the load is stored in the supercap, and the "dc–dc Battery" converter is still disabled. This stage lasts until the capacitor reaches 1.9 V, when a sufficient energy is stored for start charging the battery: in fact if there are input power fluctuations the energy stored in the supercap should help the system to provide a constant current for the battery charging. In the "Battery Charge" stage, the input stage is still working, and MPPT implemented, but now the "dc–dc Battery" converter is enabled if the battery voltage is less than the maximum voltage: the battery can be charged with a constant current. If the voltage across the supercap is greater than the maximum voltage (2.5 V), which means that the input power is grater than the load power and the power needed to recharge the battery, the algorithm moves to the "Overvoltage" stage, where the input stage is disabled to avoid the damage of the supercap, and the battery is still in charge mode. If the supercap voltage drops below 0.9 V, then it means that the input power is not sufficient for recharging the battery and the control moves to the "Supercap Charge" stage: the battery converter is disabled; the gray stages are the only two where the battery charging can be done, this is decided according to the battery voltage: if it is low the charging phase can starts, otherwise if the voltage is near the maximum voltage the "dc–dc Battery" converter is disabled. It is preferable that the battery is fully charged in the "Overvoltage" stage so that the system will be with both storages fully recharged. The last stage is the "Battery Discharge" stage, this occurs when the supercap voltage drops below 0.8 V, and means that the input power is not enough to supply the load and the supercap is exhaust; in this phase, the battery is discharged in the dc bus at

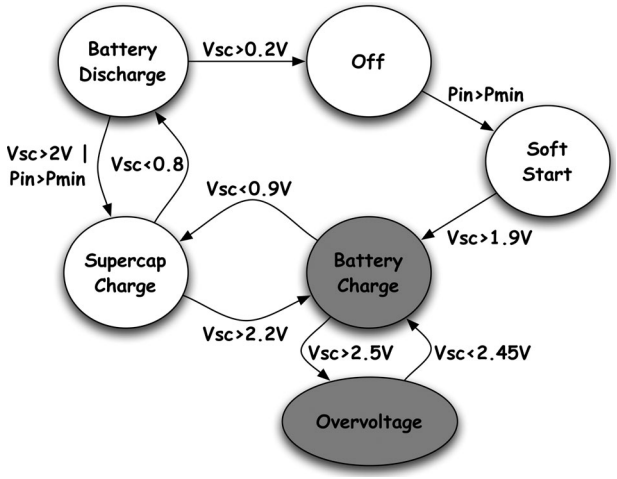

Fig. 10. Power management block diagram of the proposed solution.

a constant current and consequently the supercap is recharged until its voltage reaches 2 V or enough power at the input stage is present. If, for example, there is no input power for a long time, the systems alternates between the "Battery Discharge" stage and "Supercap Charge" until the battery and the supercap are both without energy and the system goes to "Off"

With this type of architecture and control strategy, the guidelines described in the previous paragraph for the optimal solar battery charger for increasing the lifetime of the Li-ion cells are implemented.

IV. Sources and Storages Sizing

In this type of remote applications, it is difficult to evaluate the size of the sources and storages. In some places, it is common to have several weeks without sufficient sunlight to provide energy to the remote sensor node; for this reason, the sizing should be done with a statistical approach, to ensure a certain percentage of working time of the remote system during the year.

As the penetration of PV systems is increasing, it is not difficult to obtain the historic values of their generated power; with these data, it is possible to obtain an estimation of the average power that can be generated from a certain nominal PV source in a certain place, and to simulate the behavior of a solar storage system. This paper proposes a sizing strategy based on a historical of power values of 238 days, from 8 July 2010 to 4 March 2011 of a remote sensor station, powered with a 20-W PV panel, placed near Lecco (Italy), not far from the place where the sensor network of this study will be allocated; the remote station's power supply is based on the architecture of Fig. 1(b), and monitors, as well as the environments for which it was located, the power supplied by the panel, the voltage of the storage (in this case an SLA battery) and the operating state of the converter. The power values are measured before the battery, thus the efficiency and the self-consumption of the converter were considered.

The proposed design procedure starts from the power source and the stored energy necessary to achieve a specified operating time, then it is possible to size the supercapacitor for reduce the number of charge/discharge cycles of the battery. With a MATALB–Simulink model of the architecture of Fig. 1(b), the behavior of the circuit with different loads was simulated using the historical power values mentioned earlier, and the charts in Fig. 11 were obtained; the simulated control algorithm is very simple: it charges the battery with the input power recorded data, and, if the battery voltage exceeds the maximum, the input power is switched OFF. This result is very interesting and shows that at low power loads, the operating time depends almost uniquely on the size of the storages; in our case, the consumption of the wireless sensor is 0.3 W with a duty cycle of 5 min/h, which is equivalent to an average power of 0.025 W, but the consumption of the two bidirectional converters has to be added; the overall load is estimated to be about 0.05 W.

In our application an operating time of 88–90% is sufficient so a 5-W solar panel, and a 10 kJ storage is sufficient to supply the sensor, which is equivalent to a Li-ion battery of about 700 mAh; a commercial battery for mobiles of 680 mAh has been chosen, the PV module instead has a nominal power of 5 W, a open circuit voltage of 6.6 V, and a short circuit current of 904 mA. Note that the same amount of energy stored can be obtained with a supercap of about 3000 F, but this solution would be very expensive and cumbersome.

The next step is to size the supercapacitor; a detailed Simulink model of our architecture has been developed, and controlled by a state machine that implements the control algorithm explained in the previous paragraph in order to simulate the entire system and estimate the charge/discharge cycles saved. To make the model as real as possible, several factors were considered: first, the converter efficiency was set at 80%, the internal resistance of the battery that dissipates energy, the supercap leakage current, set at 1 mA, and the autoconsumption of each converter was estimated to be about of 0.07 W with the real components used in the prototype, consumption that obviously was considered only when the converter is active. The supercap converter is the only one that works for all the time, and is designed to operate in light load conditions with a pulsed frequency modulation, to reduce the auto consumption and increase the efficiency; this feature is implemented in the model. Another nonideal factor considered is the absence of the constant voltage phase during the charge process; thus, as previously discussed, a 15% of the available capacity of the battery has not been used; the charge current instead is set at 300 mA (less than half the C rating), and the discharge current at 150 mA.

With this model, it has been possible to simulate the number of charge/discharge cycles of the battery, as defined in (1), varying the capacity of the supercap, obtaining the Fig. 12. In our application, a capacity of 1050 F has been chosen (three caps of 350 F), obtaining in the simulation an equivalent average load of about 37 mW (neglecting che auto discharge of the supercapacitors), a simulated operating time of 89.28% and an equivalent number of charge/discharge cycles of 18. The waveforms of the 238 day's simulation are reported in Fig. 13: the first image represents the overall load of the circuit and includes all the losses and the autoconsumption of the converters, as previously explained, note that the consumption of the wireless sensor is 0.3 W with a duty cycle of 5 min/h; the second image represents

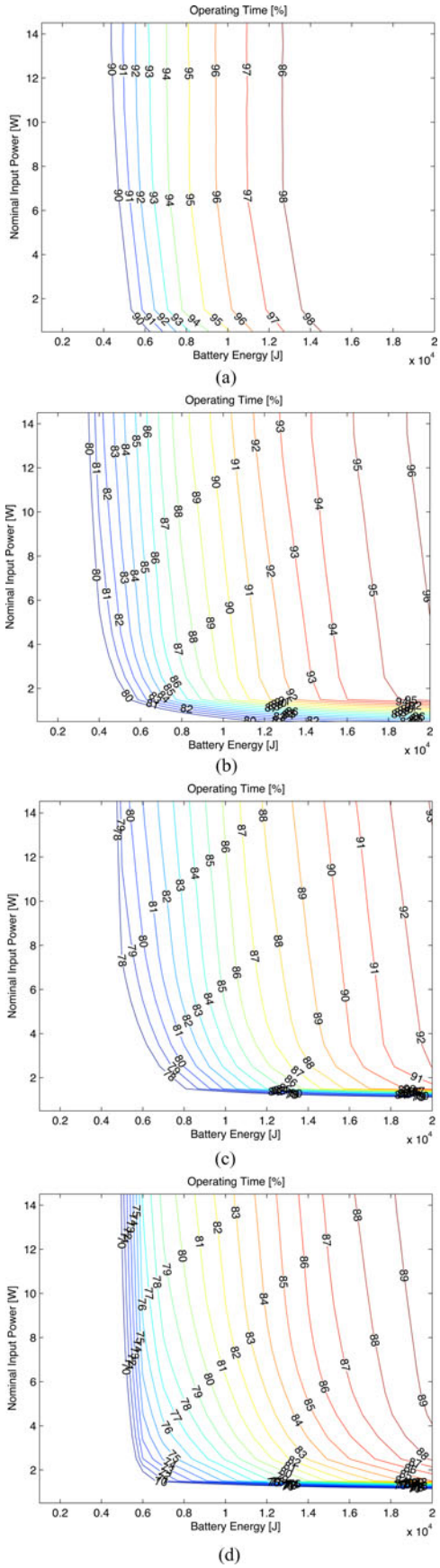

Fig. 11. Simulated operating time of the circuit in Fig. 1(b), in function of the PV nominal input power and battery energy, with a constant load of (a) 0.025 W, (b) 0.05 W, (c) 0.075 W, and (d) 0.1 W.

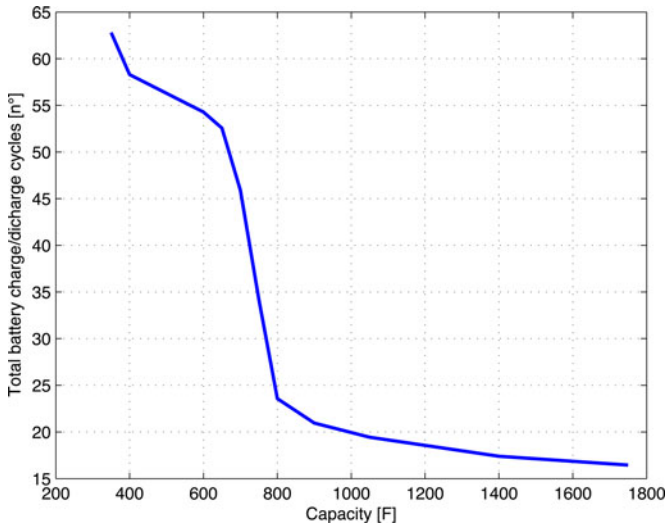

Fig. 12. Number of equivalent charge/discharge cycles, as defined in (1), in function of the capacity of the supercap.

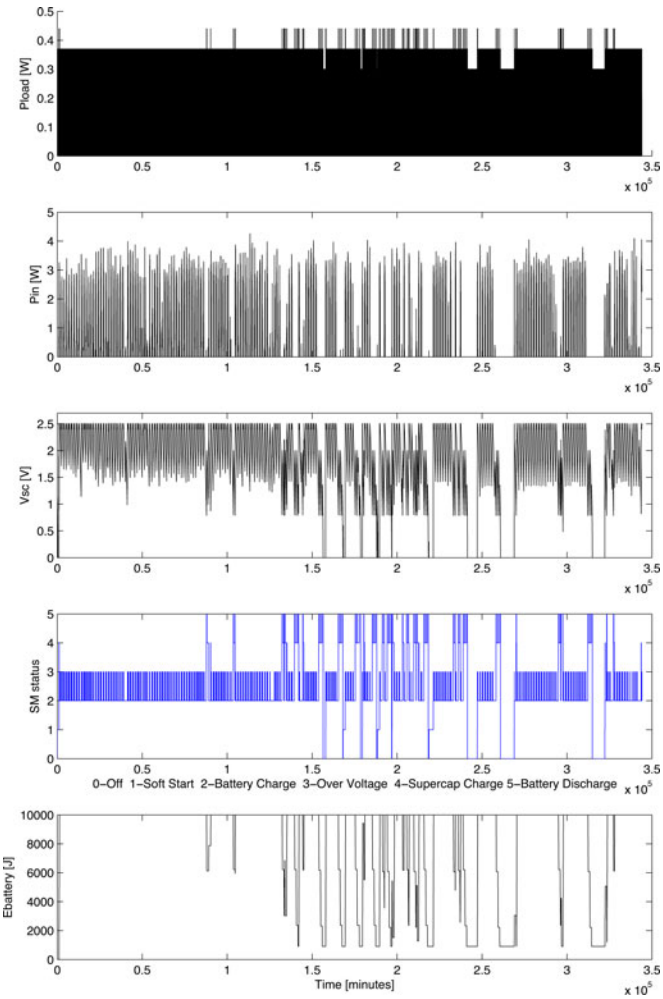

Fig. 13. Simulation of 238 days of the proposed architecture, with a solar source of 5 W, a supercap of 1050 F and a Li-ion battery of 680 mAh.

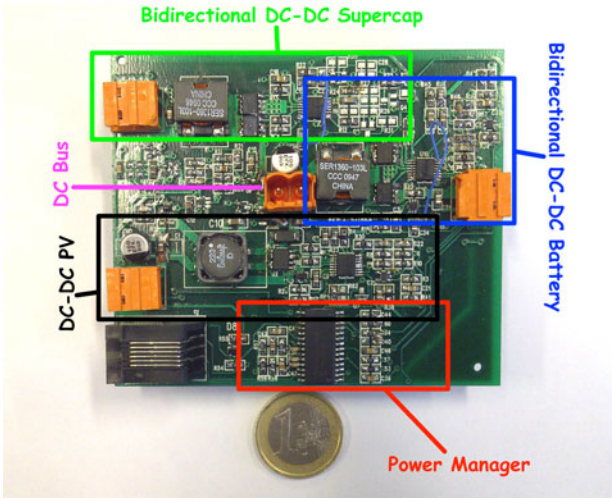

Fig. 14. Prototype of the proposed power management system.

the instantaneous input power of the solar panel; the third image is the supercap voltage; the fourth image is the status of the control state machine, for simplicity the states are numbered: 0 is the Off state, 1 is the Soft Start state, 2 the Battery Charge state, 3 the Over Voltage state, 4 the Supercap Charge state, and 5 is the Battery Discharge state, coherent with Fig. 10; and the last figure is the total instantaneous energy of the battery. Considering the same average load in the Simulink model of Fig. 1(b), used for sizing the battery, the number of charge/discharge cycles applied to the battery with the traditional architecture were estimated to be about 87 cycles that means almost 4.8 times the cycles required by our architecture. The different slopes in Fig. 12 can be interpreted as follows: the greatest increase of saved charge cycles is obtained using a supercap that can supply the circuit for all the night without using the battery (as visible from the voltage battery and energy in the simulation of Fig. 13); then, the saved cycles becomes less, because the only benefit is to increase the overall storage energy and so the operating time, operation that can be made using a higher capacity battery.

V. Experimental Results

The power management system was experimentally verified on a prototype built using discrete component off the shelf, photographed in Fig. 14. The power manager is implemented by a microcontroller of the Microchip family (PIC18F2620), and it works with a quartz crystal oscillator of 4 Mhz for reduce the consumption. The controller utilized for each of the tree converters is a TPS43000; the sepic converter is realized with a coupled inductor from Coilcraft MSD1278, of $10\,\mu$H, the two MOSFETs are a FDS9934C and operates at a switching frequency of 250 kHz.

The two bidirectional converters work at the same frequency, which is 490 kHz and the inductors are SER1360 of 10 μH each, produced by Coilcraft: these choices were made to reduce the current ripple and the switching losses at low loads; the high side MOSFETs are IRF7433 and the low sides MOSFETs are IRF1902, both driven directly from the internal driver of

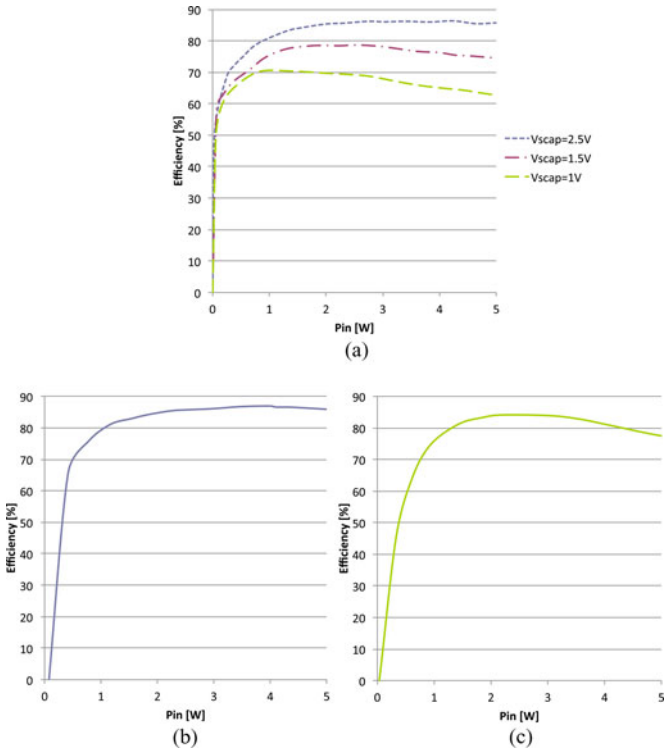

Fig. 15. Efficiencies of the three main converters: (a) is the measured efficiency of the bidirectional dc–dc Supercap converter in Buck mode, at different supercap voltages (b) is the measured efficiency of the bidirectional dc–dc Battery and (c) is the measured efficiency of the dc–dc PV converter.

the TPS43000; infact MOSFETs with a low total gate charge Q_g are chosen to reduce the driving losses. Two current senses are needed to implement the algorithm previously described, one on the input source for measure the instantaneous power of the solar module, and another to measure the battery current, both realized with an INA213. The supercaps are three Maxwell Boostcap CCAP0350, of 350 F and the battery is a simple Li-ion battery for mobiles, a Cellular Line BSIV3, 3.7 V, 680 mAh.

The efficiencies of the three main converters are reported in Fig. 15(a)–(c): the measured efficiency of the bidirectional dc–dc Supercap converter in buck mode, at different supercap voltages; the measured efficiency of the bidirectional dc–dc battery; and the measured efficiency of the dc–dc PV converter, respectively. In order to verify the correct operation of the circuit, an SPI interface has been connected to the power manager; this comunication enables the monitoring of currents and voltages in the circuit and of the state of the power manager, as well as the verification of the validity of the Simulink model and the proposed design procedure. The sampled values are reported in Fig. 16: the first image represents the solar panel voltage, the second image represents the instantaneous input current of the solar panel, the third image is the instantaneous input power, the fourth image is the voltage across supercap, the fifth image is the status of the control state machine, for simplicity the states are numbered: 0 is the Off state, 1 is the Soft Start state, 2 the Battery Charge state, 3 the Over Voltage state, 4 the Supercap Charge state, and 5 is the Battery Discharge state, coherently with Fig. 10; and the last figure is the voltage of the battery.

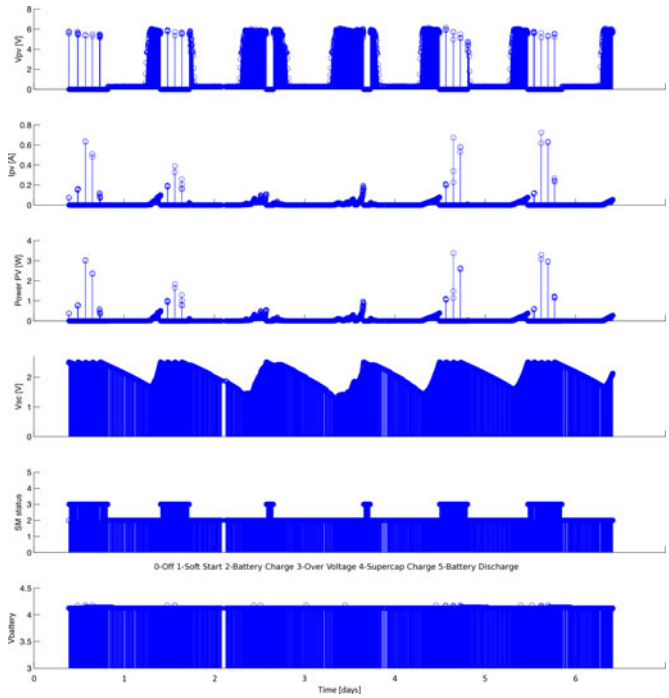

Fig. 16. Measured voltages, currents, and state variables of the circuit prototype after a period of 6 days.

To verify the operating time of the circuit, several months of measures in the wireless sensor network's position are required, measures that are not available; to verify our model, however, it is sufficient to evaluate the voltage ripple of the supercap during several nights: if during the day the supercap is fully charged, in the night the voltage should drop at values similar to those obtained using the simulation model. From the simulation of Fig. 13, the voltage of the supercap during the night drops to about 1.5/1.8V, as in the measured values of Fig. 16: this confirms the accuracy of the simulation model and the validity of the proposed design procedure.

VI. Conclusion

This paper has investigated a power management architecture that utilizes both supercapacitor cells and a Li-ion battery as energy storages for a PV-based wireless sensor network. The proposed architecture shows that a combination of both energy storage elements reduces the number of charge/discharge cycle of the Li-ion battery, improving the battery lifetime. In order to size the energy storage elements, a statistical approach based on historical power data has been proposed. Simulation results show that the charge/discharge battery cycles are reduced almost by a factor 4. The experimental results have validated the design procedure for sizing the storages and shown good agreement with the simulation model, although in a shorter time scale. While the proposed power management architecture and statistical design approach may have a potential broad application, the specific circuit prototype faces to major limitations: the auto consumption of the supercap converter, being 37 mW the average absorbed power and 25 mW the one required by the sensor, and the efficiency at low load. A controller that implements a pulsed frequency modulation is almost necessary, and using a high value of inductance can increase the efficiency at light loads.

References

[1] N. Guilar, A. Chen, T. Kleeburg, and R. Amirtharajah, "Integrated solar energy harvesting and storage," in *Proc. Int. Symp. Low Power Electron. Design*, Oct. 4–6, 2006, pp. 20–24.

[2] V. Raghunathan, A. Kasal, J. Hsu, J. Friedman, and M. Srivastava, "Design consideration for solar energy harvesting wireless embedded system," in *Proc. IEEE Int. Conf. Inf. Process. Sens. Netw.*, Apr. 15, 2005, pp. 457–452.

[3] K. Liu and J. Makaran, "Design of a solar powered battery charger," in *Proc. IEEE Electr. Power Energy Conf.*, 2009, pp. 1–5.

[4] D. C. Riawan and C. V. Nayar, "Analysis and design of a solar charge controller using CUK converter," in *Proc. Aust. Univ. Power Eng. Conf.*, Dec. 9–12, 2007, pp. 1–6.

[5] D. Brunelli, C. Moser, L. Thiele, and L. Benini, "Design of a solar-harvesting circuit for batteryless embedded systems," *IEEE Trans. Circuits Syst.*, vol. 56, no. 11, pp. 2519–2528, Nov. 2009.

[6] S. S. Choi and H. S. Lim, "Factors that affect cycle-life and possible degradation mechanisms of a Li-ion cell based on LiCoO2," *J. Power Sources*, vol. 111, no. 1, pp. 130–136, 2002.

[7] S. Kim, P. Ji, U. D. Han, C. G. Lhee, and H. G. Kim, "State estimator design for solar battery charger," in *Proc. IEEE Int. Conf. Ind. Technol.*, 2009, pp. 1–6.

[8] L.-R. Chen, R. C. Hsu, and C.-S. Liu, "A design of a grey-predicted li-ion battery charge system," *IEEE Trans. Ind. Electron.*, vol. 55, no. 10, pp. 3692–3701, Oct. 2008.

[9] B. Carter, J. Matsumoto, A. Prater, and D. Smith, "Lithium ion battery performance and charge control," in *Proc. Energy Convers. Eng. Conf.*, 1996, pp. 363–368.

[10] J. Qian and S. Wen, "Power electronics in battery powered applications: Safety, monitoring, charging and power conversion," in *Proc. Appl. Power Electron. Conf. Professional Semin.*, 2010, pp. 1–123.

[11] S. Y. Kan, M. Verwaal, and H. Broekhuizen, "The use of batterycapacitor combinations in photovoltaic powered products," *J. Power Sources*, vol. 162, pp. 971–974, 2006.

[12] Maxwell K2 Ultracap Datasheet, [Online]. Available: http://www.maxwell.com/docs/DATASHEET_K2_SERIES_1015370.PDF

[13] M. E. Glavin, P. K. W. Chan, S. Armstrong, and W. G. Hurley, "A stand-alone photovoltaic supercapacitor battery hybrid energy storage system," in *Proc. Power Electron. Motion Control Conf., EPE-PEMC 2008*, pp. 1688–1695.

[14] C. Alippi and C. Galperti, "Energy storage mechanisms in low power embedded systems: Twin batteries and supercapacitors," in *Proc. Int. Conf. Wireless Comun., Veh. Tecnol., Inf. Theory Aereosp. Electron. Syst. Technol.*, May 17–20, 2009, pp. 31–35.

[15] Y. S. Lee and G. T. Cheng, "Quasi-resonant zero-current-switching bidirectional converter for battery equalization applications," *IEEE Trans. Power Electron.*, vol. 21, no. 5, pp. 1213–1224, Sep. 2006.

[16] D. Lei, W. Xueping, L. Zhen, and L. Xiaozhong, "A new soft switching bidirectional buck or boost DC-DC converter," in *Proc. Int. Conf. Electr. Mach. Syst.*, 2008, pp. 1163–1167.

[17] A. Mirzaei, A. Jusoh, Z. Salam, E. Adib, and H. Farzanehfard, "Analysis and design of a high efficiency bidirectional DC-DC converter for battery and ultracapacitor applications," in *Proc. IEEE Int. Conf. Power Energy*, 2010, pp. 803–806.

[18] W. S. Liu, J. F. Chen, T. J. Liang, R. L. Lin, and C. H. Liu, "Analysis, design, and control of bidirectional cascoded configuration for a fuel cell hybrid power system," *IEEE Trans. Power Electron.*, vol. 25, no. 6, pp. 1565–1575, Jun. 2010.

[19] J. A. Paradiso and T. Starner, "Energy scavenging for mobile and wireless electronics," *IEEE Pervas. Comput.*, vol. 4, no. 1, pp. 18–27, Jan.–Mar. 2005.

[20] S. Saggini, F. Ongaro, C. Galperti, and P. Mattavelli, "Supercapacitor-based hybrid storage systems for energy harvesting in wireless sensor networks," in *Proc. Appl. Power Electron. Conf. Expos.*, Feb. 21–25, 2010, pp. 2281–2287.

[21] A. F. Burke, "Batteries and ultracapacitors for electric, hybrid, and fuel cell vehicles," *Proc. IEEE*, vol. 95, no. 4, pp. 806–820, Apr. 2007.

[22] R. W. Erickson and D. Maksimovic, *Fundamentals of Power Electronics*, 2nd ed. New York: Springer-Verlag, 2001, pp. 52–56, 92–101.

Fabio Ongaro received the M.S. degree in electronic engineering from the University of Udine, Udine, Italy, in 2009, where he is currently working toward the Ph.D. degree in information engineering.

From 2009 to 2010, he was a Temporary Research Assistant in the Polytechnic of Milan, Milan, Italy, where he has researched on power solutions for remote sensor networks. In 2011, he was with CERN of Genéve, Switzerland, researching and developing radiation tolerant integrated dc–dc converters. He is currently with the Texas Instruments Incorporated, Freising, Germany, developing low power dc–dc converters and solutions.

Stefano Saggini received the M.S. degree in electronic engineering and the Ph.D. degree in information engineering from the Politecnico di Milano, Milano, Italy, in 2000 and 2004, respectively.

He joined STMicroelectronics, Industrial and Power Supply Division, in 2004. Since December 2006, he has been with the Department of Electrical, Mechanical and Management Engineering, University of Udine, Udine, Italy. His research interests include modeling, control, and digital control techniques for power systems.

Dr. Saggini received the Prize Paper Award for the IEEE TRANSACTIONS ON POWER ELECTRONICS in 2004.

Paolo Mattavelli (S'95–A'96–M'00–SM'11) received the Laurea degree (with Hons.), and the Ph.D. degree in electrical engineering from the University of Padova, Padova, Italy, in 1992 and 1995, respectively.

From 1995 to 2001, he was a Researcher at the University of Padova. From 2001 to 2005, he was an Associate Professor in the University of Udine, where he led the Power Electronics Laboratory. In 2005, he joined the University of Padova, Vicenza, Italy, with the same duties. Since 2010, he has been with Virginia Tech as a Professor and member of the Center for Power Electronics Systems. His major field of interest includes analysis, modeling and control of power converters, digital control techniques for power electronic circuits, and grid-connected converters for power quality and renewable energy systems. In these research fields, he has been leading several industrial and government projects.

Dr. Mattavelli has served as an Associate Editor for IEEE TRANSACTIONS ON POWER ELECTRONICS in 2003. From 2005 to 2010, he was the Industrial Power Converter Committee Technical Review Chair for the IEEE TRANSACTIONS ON INDUSTRY APPLICATIONS. For session 2003–2006 and 2006–2009, he was also a member-at-large of the IEEE Power Electronics Society's Administrative Committee. He also received the Prize Paper Award in the IEEE TRANSACTIONS ON POWER ELECTRONICS in 2005 and 2006, and a second place in the Prize Paper Award at the IEEE Industry Application Annual Meeting in 2007.